Fish and Shellfish Immunology 92 (2019) 460–468

Contents lists available at ScienceDirect

Fish and Shellfish Immunology

journal homepage: www.elsevier.com/locate/fsi

Full length article

Cloning and characterization of the target protein subunit lst8 of rapamycin in *Apostichopus japonicus*

Zongxu Yue[a], Zhimeng Lv[a], Yina Shao[a], Weiwei Zhang[a], Xuelin Zhao[a], Ming Guo[a], Chenghua Li[a,b,*]

[a] State Key Laboratory for Quality and Safety of Agro-products, Ningbo University, Ningbo, 315211, PR China
[b] Laboratory for Marine Fisheries Science and Food Production Processes, Qingdao National Laboratory for Marine Science and Technology, Qingdao, 266071, PR China

ARTICLE INFO

Keywords:
Apostichopus japonicus
Lethal with SEC13 protein 8
Gene expression
Gene interference
Autophagy

ABSTRACT

Autophagy plays an important role in the immune defense systems of vertebrates through the interaction between the lethal with SEC13 protein 8 (lst8) and the mechanistic target of rapamycin. In the present study, a novel invertebrate lst8 homologue is identified from *Apostichopus japonicus* (designated as *Ajlst8*) via polymerase chain reaction. The full-length complementary DNA of *Ajlst8* comprises a 5′-untranslated region (UTR) of 78 base pair (bp), a 3′-UTR of 479 bp, and a putative open reading frame of 951 bp; hence, 316 amino acids are encoded. Structural analysis shows that the deduced amino acid of Ajlst8 shares six typical WD40 domains (28 aa–248 aa). Spatial expression analysis indicates that *Ajlst8* is ubiquitously expressed in all the examined tissues, with a larger magnitude in coelomocytes. *Vibrio splendidus* infection *in vivo* and lipopolysaccharide exposure *in vitro* can significantly upregulate the messenger RNA expression of *Ajlst8* by 2.39-fold and 1.93-fold compared with the control group, respectively. LPS exposure could also significantly induced the protein level of Ajlst8 to 2.38-fold and the autophagy level was markedly increased by 3.08-fold under same condition. The RNA interference of Ajlst8 in primary coelomocytes also reduces the relative expression of autophagy with a 0.71-fold decrease in the ratio of LC3-II/LC3-I compared with that in the control group. These results indicate that Ajlst8 is a novel immune regulator that may be involved in the antibacterial response process of sea cucumber by regulating autophagy.

1. Introduction

Autophagy is a critical process for recycling cytoplasmic materials during nutrient deprivation, environmental stress, senescence, and cellular remodeling; it has been widely reported from yeast to mammals [1–4]. An increasing number of studies have also shown that autophagy is involved in well-balancing inflammatory response and functions as a primordial form of eukaryotic innate immunity [5]. The mechanistic target of rapamycin complex 1 (mTORC1) is well-accepted as an autophagy-associated protein and has been intensively investigated in model animals and fish [6,7]. mTORC1 serves as the primary gateway to autophagy by regulating Unc-51 like autophagy activating kinase 1 (ULK1) and autophagy initiation [8,9]. Many important signaling pathways, including PI3K/Akt, AMPK, and extracellular signal-regulated kinase, ultimately regulate cellular autophagy [10,11]. Although the role of mTORC1 as a key signal factor in activating autophagy has been accepted, the different components of mTORC1 involved in autophagy have not been well-documented.

The essential core components of mTORC1 consist of the mechanistic target of rapamycin (mTOR), regulatory-associated protein of mTOR (raptor), and the lethal with SEC13 protein 8 (lst8) [12]. As a scaffolding protein, the accessory protein lst8 is essential for mTORC1 kinase activity and the stability of raptor–mTOR [13–15]. In *Drosophila*, lst8 influences Atg13 phosphorylation levels and the dephosphorylation of Atg13 to facilitate its interaction with Atg1 or Atg17 and the induction of autophagy [16,17]. Chen et al. indicated that the complete depletion of lst8 may eventually cause mTORC1 disintegration and modulate innate immune defense in humans [18]. The knockdown of lst8 prevents mTORC formation and inhibits tumor growth and invasiveness [19]. Simultaneously, autophagy dysfunction is an increasingly recognized modulator of disease onset and progression; it is likely important as a functional autophagy pathway in cancer prevention [20,21].

As a highly conserved cell immune function [22], autophagy has also been reported in invertebrates, such as *Caenorhabditis elegans* [6] and *Drosophila melanogaster* [23]. Autophagy plays a protective role in

* Corresponding author. 818 Fenghua Road, Ningbo University, Ningbo, Zhejiang Province, 315211, PR China.
E-mail address: lichenghua@nbu.edu.cn (C. Li).

https://doi.org/10.1016/j.fsi.2019.06.038
Received 11 May 2019; Received in revised form 14 June 2019; Accepted 17 June 2019
Available online 21 June 2019

flies infected with the obligate intracellular Gram-negative bacterium [24]. It is also required in *D. melanogaster* defense against viral infection; moreover, the RNA interference (RNAi) knockdown of the autophagy gene in adult flies increases viral replication and decreases the survival of infected flies [25]. Jia et al. suggested that autophagy may prevent bacterium intracellular persistence and replication in *C. elegans* [26]. Although autophagy functions and molecular patterns have been extensively studied in model animals, they are rarely known in marine animals, particularly in sea cucumber, which is the key species that represents the evolutionary transition from invertebrates to vertebrates. In the current study, we use a marine echinoderm species, namely, *Apostichopus japonicus* (Echinodermata, Holothuroidea), as a model to address this issue. On the one hand, *A. japonicus* is the boundary organism between invertebrates and vertebrates in deuterostomes and is closer to chordates; it is considered an ideal model for investigating the autophagy mechanism of sea cucumber rapamycin target protein subunit lst8 [27]. On the other hand, the aquaculture of sea cucumber is one of the largest industries in China, with an annual production of approximately 220,000 tons valued at 30 billion yuan [28]. The large-scale culture of this species has led to the gradual introduction of various viral and bacterial diseases into sea cucumber aquaculture and has resulted in incalculable loss in this industry [29]. A dramatic decline in wild *A. japonicus* population has been observed recently in China due to the outbreaks of infectious diseases [30], such as skin ulceration syndrome, which is the most contagious and lethal disease in the sea cucumber culture industry [31]. To improve the understanding of disease outbreaks, we cloned the full-length complementary DNA (cDNA) of *Ajlst8* from *A. japonicus* in the current study and then investigated its spatial- and time-course expression patterns. The functional characterization of Ajlst8 in regulating coelomocyte autophagy was also explored through RNAi. The results of this study can be used to elucidate the complex mechanism of the autophagy pathway in sea cucumber. Understanding the molecular mechanisms of molecules, such as lst8, may improve the health management and disease control of aquaculture species.

2. Materials and methods

2.1. Experimental animals

Healthy adult *A. japonicus* individuals, weighing 120 ± 11 g, were collected from the Dalian Pacific Aquaculture Company and acclimatized in aerated seawater (salinity: 29 ± 1; temperature: 16 °C ± 1 °C) for 3 days. For the time-course expression analysis of *Ajlst8*, one tank was used as the control and five tanks contained fresh *Vibrio splendidus* at a final concentration of 10^7 CFU mL^{-1}. Coelomic fluids from five individuals in the control and challenged groups were collected at 0, 6, 12, 48, and 72 h postinoculation. The coelomic fluids were then centrifuged at 800 × *g* for 5 min at 4 °C to collect coelomocytes. For the spatial-course expression analysis, coelomocytes and five other tissues (i.e., muscles, tentacles, respiratory trees, body walls, and intestines) were collected from the control individuals by using sterilized scissors and tweezers. Five biological replicates were obtained from the experimental and control groups, and all samples were stored at −80 °C before RNA extraction and cDNA synthesis.

2.2. Cloning the full-length cDNA of Ajlst8

Total RNA from coelomocytes was extracted with RNAiso Plus reagent (TaKaRa Bio Inc.), and the first-strand cDNA was synthesized using Primescript™ II 1st cDNA Synthesis Kit (TaKaRa Bio Inc.) following the manufacturer's protocol. Four gene-specific primers, namely, *Ajlst8*-5-1, *Ajlst8*-5-2, *Ajlst8*-3-1, and *Ajlst8*-3-2 (Table 1), were designed on the basis of the annotated expressed sequence tag of *Ajlst8* and used to amplify the 3′ and 5′ end of *Ajlst8*. The desired polymerase chain reaction (PCR) products were cloned into a pMD19-T simple vector (TaKaRa Bio Inc.) and sequenced at Sangon Biotechnology (Shanghai).

Table 1
Primers used for cloning, quantitative real-time PCR and RNA interference.

Primer Name	Primer Sequence (5′-3′)	Used for
Ajlst8-5-1	CGTAACCAGCAGTAGCAAGA	5′ RACE
Ajlst8-5-2	CCGTCTGTCGGGAGTGATTT	
Ajlst8-3-1	GGAAGCACATCGGAAATACGCAC	3′ RACE
Ajlst8-3-2	CAGTGAAGATTTGGAAAACGGCAGA	
Ajlst8-F	GACCACACGATCCGGTTTTG	FBG amplification
Ajlst8-R	TTGACGGTTCCCTGTTCCAC	
AjLC3-F	ATGGGATCCGATTCTTCAAAGCA	
AjLC3-R	TCAATTACCGAACATTTCTTGCG	
Ajlst8-BamHI-F	GGATCCGACCACACGATCCGGTTTTG	Vector construction
Ajlst8-NotI-R	GCGGCCGCTTGACGGTTCCCTGTTCCAC	
AjLC3-EcoRI-F	GAATTCATGGGATCCGATTCTTCAAAGCA	
AjLC3-XhoI-R	CTCGAGTCAATTACCGAACATTTCTTGCG	
Ajlst8-qF	GAGGCCACGCCATTCGTATTCTC	Real-time PCR
Ajlst8-qR	TGTTTGGTCTGCTGATGTGGTGG	
Ajβ-Actin-qF	CCATTCAACCCTAAAGCCAACA	Real-time PCR
Ajβ-Actin-qR	ACACACCGTCTCCTGAGTCCAT	
Ajlst8 specific siRNA	Sense: CCGUCAAGAGGGAGUUCAATT Anti-sense: UUGAACUCCCUCUUGACGGTT	RNA interference
Negative control siRNA	Sense: UUCUCCGAACGUGUCACGUTT Anti-sense: ACGUGACACGUUCGGAGAATT	Negative control (NC) For siRNA interference

2.3. Sequence analysis of Ajlst8 cDNA

The *Ajlst8* sequence was analyzed using the BLAST algorithm of the National Center for Biotechnology Information (http://www.ncbi.nlm.nih.gov/blast). The predicted amino acid sequence was analyzed with ExPASy (http://www.expasy.org/). The percentage of sequence similarity between Ajlst8 and lst8 from other organisms was calculated using the Identity and Similarity Analysis program (http://www.biosoft.net/sms/index.html). The domain in the Ajlst8 amino acid sequence was detected using the Simple Modular Architecture Research Tool (SMART) program (http://www.smart.embl-heidelberg.de/). A phylogenetic tree was constructed on the basis of the full-length amino acid sequences of various original lst8 proteins using Mega 5.0 (http://www.megasoftware.net/).

2.4. Spatial expression analysis of Ajlst8 messenger RNA (mRNA)

The expression patterns of *Ajlst8* in the six tissues, namely, muscles, tentacles, intestines, respiratory trees, body walls, and coelomocytes, were investigated using the ABI 7500 real-time PCR detection system. Beta-actin functioned as the internal control to verify successful reverse transcription and calibrate the cDNA template. Two specific primers for *Ajlst8*, i.e., *Ajlst8*-qF and *Ajlst8*-qR (Table 1), were designed to amplify a product of 285 base pair (bp). Real-time PCR amplifications were performed in a total volume of 20 μL with 10 μL 2 × SYBR Green Mix (TaKaRa Bio Inc.), 8 μL diluted cDNA (1:20), and 1 μL of each primer (10 mM). The reaction mix was incubated for 5 min at 95 °C, followed by 40 amplification cycles of 15 s at 95 °C, and 1 min at 60 °C. The melting curve analysis of the amplified products was performed at the end of each PCR to confirm that a single PCR product was generated. The $2^{-\triangle\triangle CT}$ method was used to analyze the expression levels of *Ajlst8*, and the values represented the *n*-fold difference relative to the calibrator tissue (i.e., tentacles).

2.5. Time-course analysis of Ajlst8 in response to V. splendidus challenge

Coelomocytes were selected to analyze the temporal expression profile of *Ajlst8* in the *V. splendidus*-challenged sea cucumbers from Section 2.1. The untreated samples served as the control. Data were presented as mean ± standard deviation (SD) ($n = 5$). The results were

subjected to one-way ANOVA, followed by Duncan's multiple range tests, to determine the differences between the challenged and control groups at each sampling time. *P* values less than 0.05 were considered significantly different.

2.6. Temporal expression profiles of Ajlst8 in lipopolysaccharide (LPS)-exposed primary coelomocytes

The harvested coelomocytes were resuspended in L-15-S cell culture medium for sodium (Invitrogen, USA) with penicillin (100 U mL^{-1}) and streptomycin sulfate (100 mg mL^{-1}) at a final concentration of 10^6 cells mL^{-1}. NaCl solution was utilized to adjust the osmotic pressure to a final concentration of 0.39 M. The cells were then dispensed into a 24-well culture microplate with 500 μL L-15-S medium in each well. All the experiments were performed for 48 h to ensure that the cells were in a healthy adherent state. For LPS exposure, the cells were exposed to 10 μg mL^{-1} chromatographically purified LPS from *Escherichia coli* 055:B5 (Sigma) for 1, 3, 6, 12, and 24 h. The untreated cells were used as control. Three biological replicate cells were collected and dissolved in TRIzol for *Ajlst8* expression analysis.

2.7. Prokaryotic expression and polyclonal antibody generation of recombinant Ajlst8

The mature peptide of *Ajlst8* was amplified from cDNA using two primers: *Ajlst8*-BamHI-F and *Ajlst8*-NotI-R (Table 1). After restriction enzyme digestion, the product was orientally inserted into the same digested pET-28a (+) vector. The recombinant pET-28a-Ajlst8 plasmid was transformed into competent *E. coli* BL21 cells. Recombinant Ajlst8 was generated by adding IPTG to a final concentration of 0.2 mM and purified using a nickel–nitrilotriacetic acid column (QIAGEN, Hilden, Germany). The purified protein was confirmed via sodium dodecyl sulfate (SDS) polyacrylamide gel electrophoresis under reducing conditions and visualized using Coomassie Brilliant Blue R-250.

For polyclonal antibody preparation, the purified proteins were loaded into wells with 12% SDS polyacrylamide gels. Electrophoresis was performed on a Bio-Rad mini-gel apparatus at room temperature using 1 × Tris–glycine buffer [0.025 M Tris, 0.25 M glycine, and 0.1% (w/v) SDS]. The target protein was obtained using 0.25 mM KCl solution, cut into small strips, and ground with phosphate buffered saline (PBS). A 4-week-old mouse was intradermally injected with a mixture that contained 100 μg purified Ajlst8. The mouse was boosted twice with 75 μg and 50 μg protein at 1 week interval. A week after the last immunization, antiserum was harvested from the mouse's eyes and stored at −80 °C until further use. The specificity of the generated antibodies was validated via Western blotting.

2.8. Autophagy assay in LPS-exposed primary cultured coelomocytes

For LPS-mediated cell autophagy assay, the coelomocytes from Section 2.6 were collected. These cells were exposed to LPS for 1 h and washed with PBS twice before dissolving in lysis buffer. The total protein from the coelomocytes was extracted using a Total Protein Extraction Kit (Sangon). The concentration was obtained with a BCA Protein Assay Kit (Sangon). Coelomocyte autophagy was determined on the basis of the ratio of AjLC3-II/AjLC3-I via Western blotting. Approximately 50 μg proteins were run on 10% SDS–polyacrylamide gel and transferred onto 0.45 μm enhanced chemiluminescence (ECL) membranes. After blocking with 5% skimmed milk in TBST (50 mmol L^{-1} Tris–HCl, 150 mmol L^{-1} NaCl, and 1% Tween 20) at room temperature for 120 min, the membranes were incubated with antibodies diluted at 1:500 in 5% bovine serum albumin (BSA) solution at 4 °C overnight. The antisera of Ajlst8 and AjLC3 were prepared in accordance with Section 2.7. The membranes were incubated with horseradish peroxidase-labeled anti-rat IgG (1:2000) in 5% BSA solution at room temperature for 1.5 h. The membrane was incubated in Western Lightning ECL substrate (PerkinElmer, Inc.) prior to exposure to X-OMAT AR X-ray film (Eastman Kodak, Rochester, NY). The protein bands were quantified using ImageJ software package, and the results were derived from the statistical analysis of three independent experiments.

2.9. Functional analysis of Ajlst8-mediated coelomocyte autophagy by small interfering RNA (siRNA)

siRNA that targeted Ajlst8 was synthesized at Shanghai GenePharma (China) (Table 1). For the transfection experiment, 1 μL *Ajlst8*-specific siRNA duplex (20 μM) or the negative control (20 μM) was mixed with 1 μL Mate transfection reagent (GenePharma). The mixture was then transfected into 500 μL primary cultured cells in each well. The cells were washed with cold PBS and then centrifuged at 800 × *g* and 4 °C for 5 min after transfection for 24 h to harvest coelomocytes. Three biological replicate cells were collected for further analysis. The RNAi efficiency of *Ajlst8* was determined via quantitative real-time PCR. Coelomocyte autophagy was assayed following the description in Section 2.8.

2.10. Key resources table

Resource	Source	Identifier
Antibodies		
HRP-labeled anti-rat IgG		
ß-actin		
Chemical		
amino acid		
Glycine		
I–F		
NaCl		
nickel		
nitrilotriacetic acid		
penicillin		
sodium		
sodium dodecyl sulfate		
streptomycin sulfate		
Tris		
Tris-Glycine		
Tris-HCl		
ProteinPeptide		
Protein		
Strain		
Bl21	N/A	N/A

3. Results

3.1. cDNA cloning and sequence analysis of Ajlst8

The full-length cDNA of *Ajlst8* comprised a 5′-untranslated region (UTR) of 78 bp, a 3′-UTR of 479 bp, and a putative open reading frame (ORF) of 951 bp (Fig. 1). Hence, 316 amino acid residues were encoded with a predicted molecular weight of 35.2 kDa and a theoretical pI of 6.36. SMART analysis showed that the protein encoded by Ajlst8 shared six typical WD40 domains (distributed in 28 aa–248 aa), in which two domains were terminated by a common Trp–Asp (W–D) dipeptide. BLAST analysis indicated that Ajlst8 was highly conserved with other reported counterparts from vertebrates and invertebrates (Fig. 2). It exhibited 73.08% homology with lst8 from *Strongylocentrotus purpuratus* and 65.61% with *Homo sapiens*. The tree constructed on the basis of the lst8 encoding protein data set is shown in Fig. 3. Four lst8 proteins from vertebrates, including fish and mammals, were clustered and formed a sister group. Another sister cluster comprised 12 lst8 proteins from invertebrates. Ajlst8 was first clustered with lst8 from *S. purpuratus* (XP_786,340.1), and it formed one separate branch in the lst8 subclade. All these characteristics indicated that Ajlst8 belongs to a new

Fig. 1. Nucleotide and deduced amino acid sequence of Ajlst8. The start codon is black. The asterisk indicates the stop codon. WD40 domain sequences are underlined and highlighted in gray.

member of the invertebrate lst8 family.

3.2. Tissue expression patterns of Ajlst8

The spatial mRNA expression patterns of *Ajlst8* in different tissues are shown in Fig. 4. *Ajlst8* transcripts were detected in all the tested tissues with the lowest expression in tentacles. Compared with the expression in tentacles, the expression of *Ajlst8* transcript was slightly increased by 1.90-fold in muscles ($P < 0.05$) and 1.26-fold in body walls ($P < 0.05$). The expression levels of *Ajlst8* in the other tissues increased by 191.3-fold in intestines ($P < 0.01$) and 215.9-fold in respiratory trees ($P < 0.01$). The highest expression level was detected in coelomocytes (i.e., 426.9-fold) ($P < 0.01$).

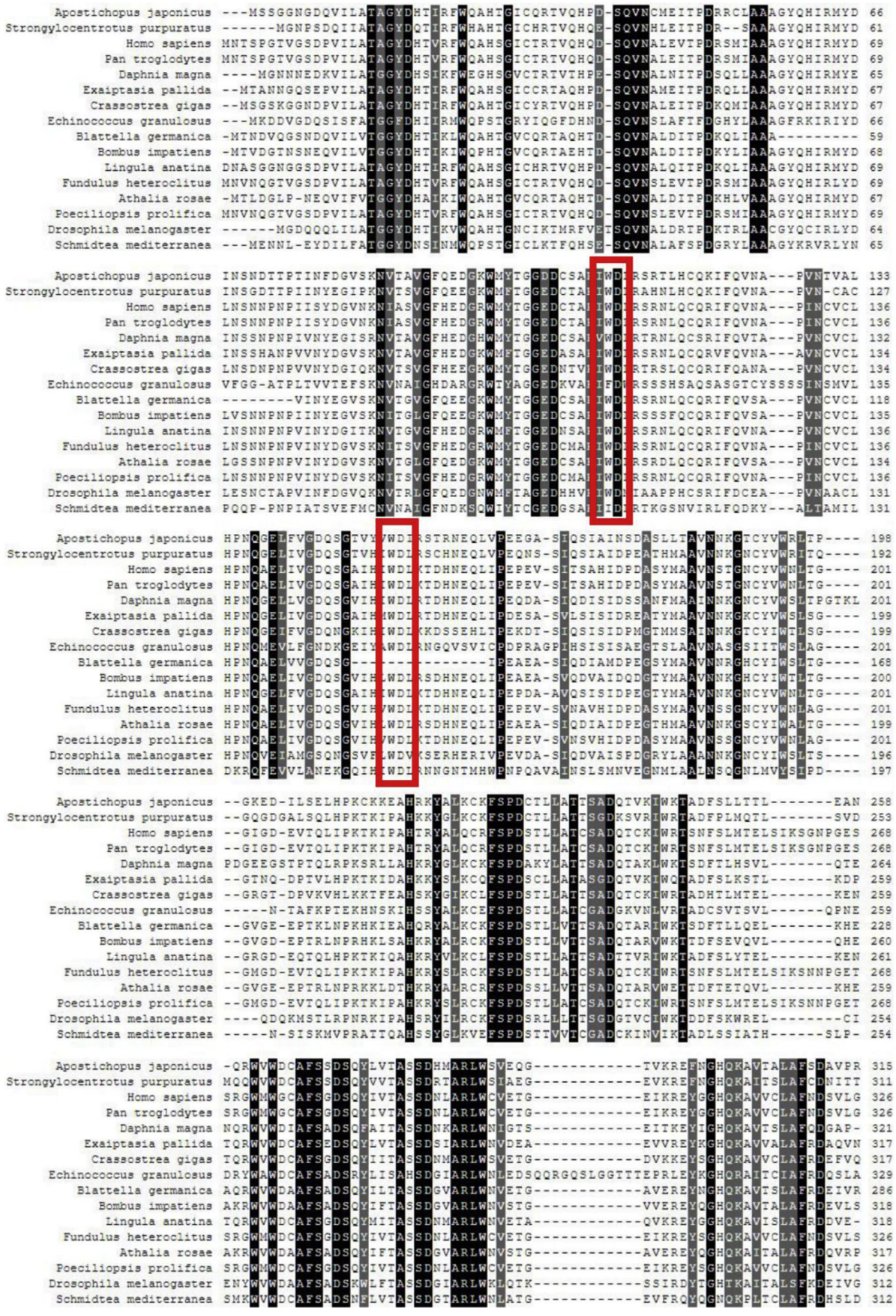

(caption on next page)

Fig. 2. Multiple sequence alignment of Ajlst8 proteins using the sequence manipulation suite. A gray shade indicates that residues are identical among all the listed lst8 proteins. The red boxes indicate amino acid residues terminating in a Trp–Asp (W–D) dipeptide. The GenBank accession numbers are as follows: *Strongylocentrotus purpuratus* (XP_786,340.1), *Homo sapiens* (XP_005255532.2), *Pan troglodytes* (XP_016784136.1), *Daphnia magna* (KZS04195.1), *Exaiptasia pallida* (KXJ27134.1), *Crassostrea gigas* (EKC35172.1), *Bombus impatiens* (XP_012240536.1), *Lingula anatina* (XP_013381964.1), *Fundulus heteroclitus* (JAR60348.1), *Athalia rosae* (XP_020708090.1), *Poeciliopsis prolifica* (JAO33818.1), *Drosophila melanogaster* (NP_572,572.1), *Schmidtea mediterranea* (AFH08799.1). (For interpretation of the references to colour in this figure legend, the reader is referred to the Web version of this article.)

3.3. Expression analysis of Ajlst8 in V. splendidus-challenged and LPS-mediated sea cucumber coelomocytes

The temporal expression levels of *Ajlst8* transcripts are shown in Fig. 5. The temporal expression of *Ajlst8* transcripts after *V. splendidus* challenge is shown in Fig. 5 A. During the first 12 h of bacterial challenge, the mRNA level of *Ajlst8* was significantly upregulated. *Ajlst8* transcripts were sharply induced and reached a peak expression level at 6 h with a 2.35-fold increase compared with the control group ($P < 0.05$). As time progressed, *Ajlst8* transcripts were slightly decreased and nearly recovered to the original level at 48 h and 72 h. A similar upregulated expression profile was detected in LPS-exposed primary cells (Fig. 5 B). An increase of 1.93-fold was observed at 1 h compared with that in the control group ($P < 0.05$). Subsequently, the expression level of *Ajlst8* gradually decreased to the original level.

3.4. LPS exposure could induce autophagy in primary cultured coelomocytes

LPS exposure could also significantly induce Ajlst8 protein level by 2.38-fold ($P < 0.01$) compared with that of the control group based on Western blot analysis (Fig. 6A). Under this condition, the ratio of LC3-II/LC3-I was also considerably increased by 3.08-fold ($P < 0.01$) (Fig. 6 B). This result indicated that coelomocyte autophagy was induced.

3.5. Ajlst8 could regulate coelomocytes autophagy via siRNA-mediated Ajlst8 silencing

To further address the regulatory correlation between Ajlst8 expression and coelomocyte autophagy, we investigated the changes in coelomocyte autophagy activities *in vitro* after *Ajlst8* interference (Fig. 7). After transfection of siRNA for 24 h, the expression of *Ajlst8* was dramatically reduced by 0.55-fold at the mRNA level ($P < 0.05$) and 0.62-fold at the protein level ($P < 0.05$). Correspondingly, the ratio of LC3-II/LC3-I was slightly decreased to 0.71-fold ($P < 0.05$) compared with that of the control group.

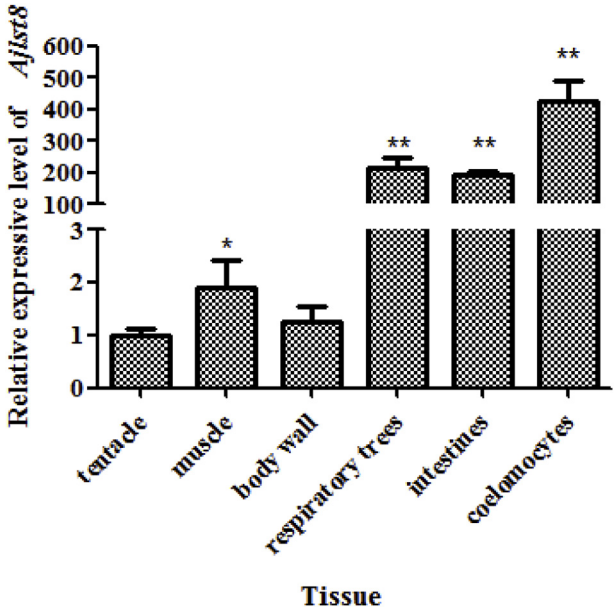

Fig. 4. Real-time PCR analysis of *Ajlst8* mRNA expression levels in the different tissues. The expression levels of *Ajlst8* mRNA among the different tissues are normalized to tentacle. Vertical bars represent the means ± SD (n = 5). Asterisks indicate significant differences: $^{**}P < 0.01$, $^{*}P < 0.05$.

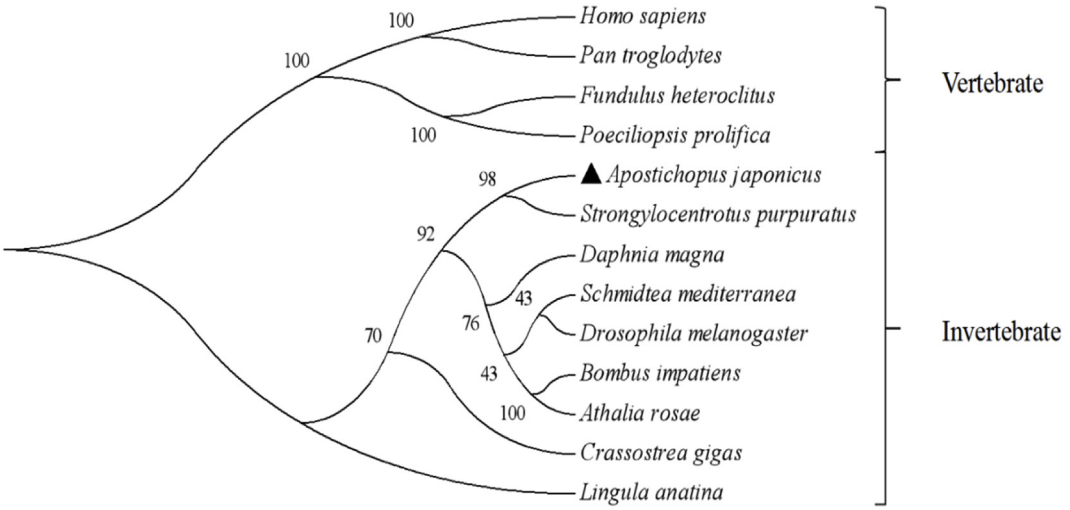

Fig. 3. An N–J phylogenetic tree based on the amino acid sequences of known Ajlst8 from original species. The tree was obtained via bootstrap analysis using the neighbor-joining method. The numbers at the forks indicate the bootstrap value. The accession numbers of these proteins from GenBank are as follows: *Strongylocentrotus purpuratus* (XP_786,340.1), *Homo sapiens* (XP_005255532.2), *Pan troglodytes* (XP_016784136.1), *Daphnia magna* (KZS04195.1), *Exaiptasia pallida* (KXJ27134.1), *Crassostrea gigas* (EKC35172.1), *Echinococcus granulosus* (XP_024350284.), *Blattella germanica* (PSN45751.1), *Bombus impatiens* (XP_012240536.1), *Lingula anatina* (XP_013381964.1), *Fundulus heteroclitus* (JAR60348.1), *Athalia rosae* (XP_020708090.1), *Poeciliopsis prolifica* (JAO33818.1), *Drosophila melanogaster* (NP_572,572.1), *Schmidtea mediterranea* (AFH08799.1).

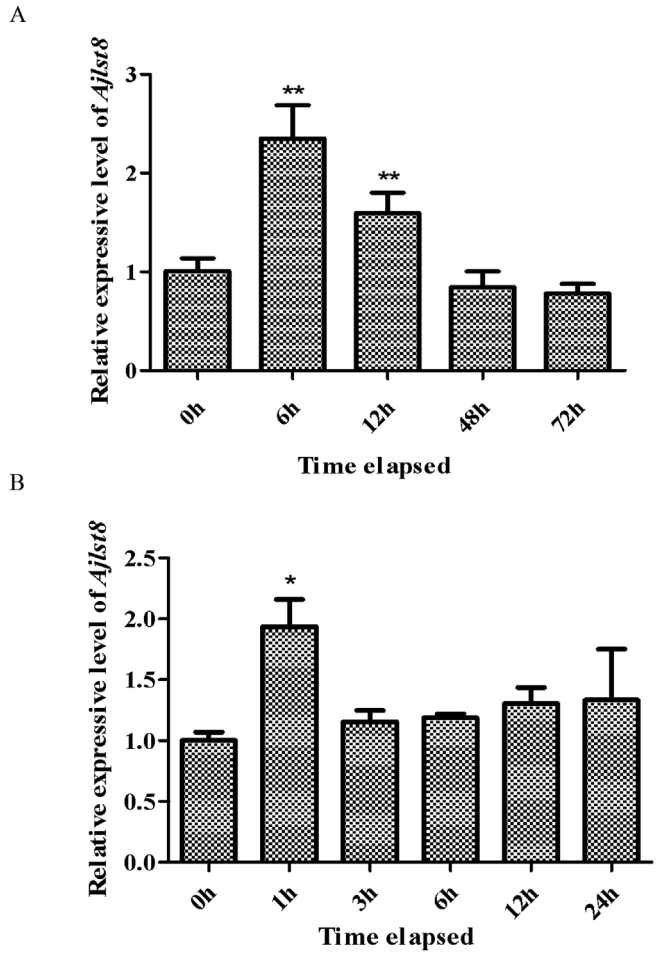

Fig. 5. Time-course expression of Ajlst8 *in vitro* and *in vivo*. A: *V. splendidus*-challenged sea cucumber. B: LPS-exposed coelomocytes. Vertical bars represent the mean ± SD (n = 3). Asterisks indicate significant differences: $^{**}P < 0.01$, $^{*}P < 0.05$.

4. Discussion

Lst8 is an mTORC1 subunit that plays crucial roles in cell autophagy, promotion of autophagosome formation, and simultaneous cell degradation in vertebrates [32]. However, the functional role of lst8 in invertebrates, particularly in immune regulation, remains largely unknown. In this study, a complete cDNA sequence of lst8 was obtained from *A. japonicus*, and its role in innate immune response was investigated. We found that the structure of Ajlst8 consists almost entirely of six typical WD40 repeats with high sequence similarity to several known lst8 proteins [33]. WD40 domain constitutes one of the most abundant protein families in eukaryotes, and frequently serves as scaffolds in assembling functional complexes by interacting with other macromolecules [34]. Ajlst8 has two domains that terminate in the conserved Trp–Asp (W–D) module; this feature contributes to the thermal stability of protein geometry [35]. WD40 repeats can form a stable propeller-like platform for the assembly of mTOR complexes or for interplay with other proteins, such as Kog1 and target of rapamycin (TOR) [36,37]. These characteristics were also detected in lst8 from other animals, such as mice [38] and planarians [39]. Furthermore, phylogenetic analysis supported that lst8 from *A. japonicus* and *S. purpuratus* form one branch in the invertebrate group. This result indicates that Ajlst8 is phylogenetically closest to its sea urchin counterpart. All these conserved characteristics and high similarity to known lst8 collectively support that Ajlst8 belongs to a new member of invertebrate lst8 family.

To uncover possible biological roles of the *Ajlst8* gene, we investigated its mRNA expression level in different tissues via quantitative real-time PCR. In this study, the mRNA transcripts of *Ajlst8* were expressed in coelomocytes, respiratory trees, muscle, and intestines. Thus, *Ajlst8* had a broad distribution in multiple tissues, with the highest expression level of *Ajlst8* observed in coelomocytes (Fig. 4). As echinoderms, sea cucumbers rely on innate immunity to identify and kill pathogens because they lack an acquired immune system [40]; such immunity is analogous to that of hemocytes and can eliminate microbial pathogens via autophagy [5]. The highest expression level of *Ajlst8* in coelomocytes suggested its important role in sea cucumber immune responses, such as autophagy, and indicated that coelomocytes may be the primary organ with lst8 involved in autophagy processes.

In vertebrates, lst8-mediated autophagy is activated by danger-associated molecular patterns, such as exogenous microbial stimuli and several viruses and bacteria in immune cells [41]. The coelomocytes of sea cucumbers is the primary tissue for *Ajlst8* expression and can efficiently eradicate the source of infection, such as immune cells in vertebrates, particularly Gram-negative pathogenic bacteria in the marine environment [42]. Hence, investigating the expression pattern of lst8 in *A. japonicus* coelomocyte response to pathogen infection is interesting. *Ajlst8* mRNA transcripts were significantly activated not only in *V. splendidus*-challenged sea cucumbers but also in LPS-exposed cultured coelomocytes (Fig. 5). The upregulated expression of *Ajlst8* was

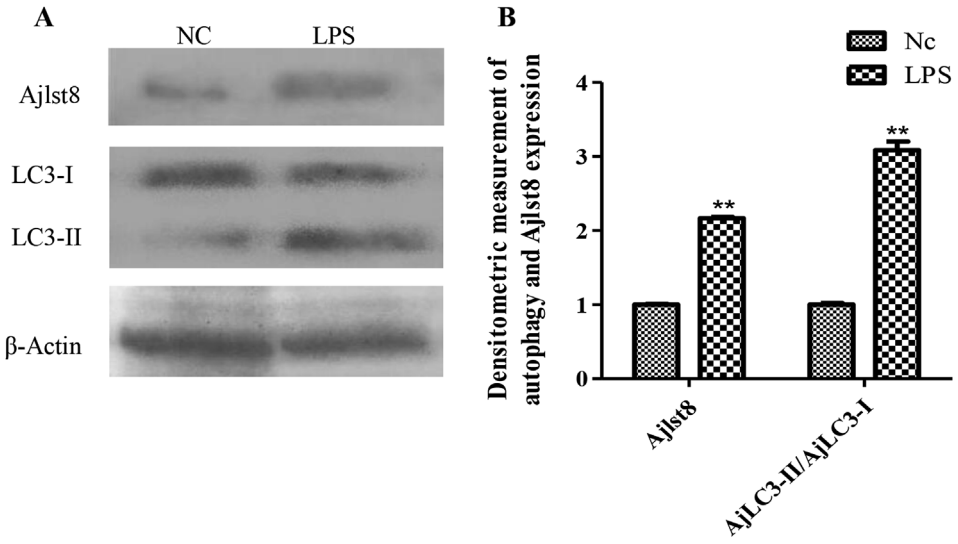

Fig. 6. Autophagy assay of primary cultured coelomocytes exposed to LPS for 1 h. A: Protein level of Ajlst8 and autophagy-related protein as determined by Western blot analysis. B: Statistical analysis of the expression levels of Ajlst8 and LC3-II/LC3-I. Values are expressed as mean ± SD ($n = 3$). Asterisks indicate significant differences: $^{**}P < 0.01$.

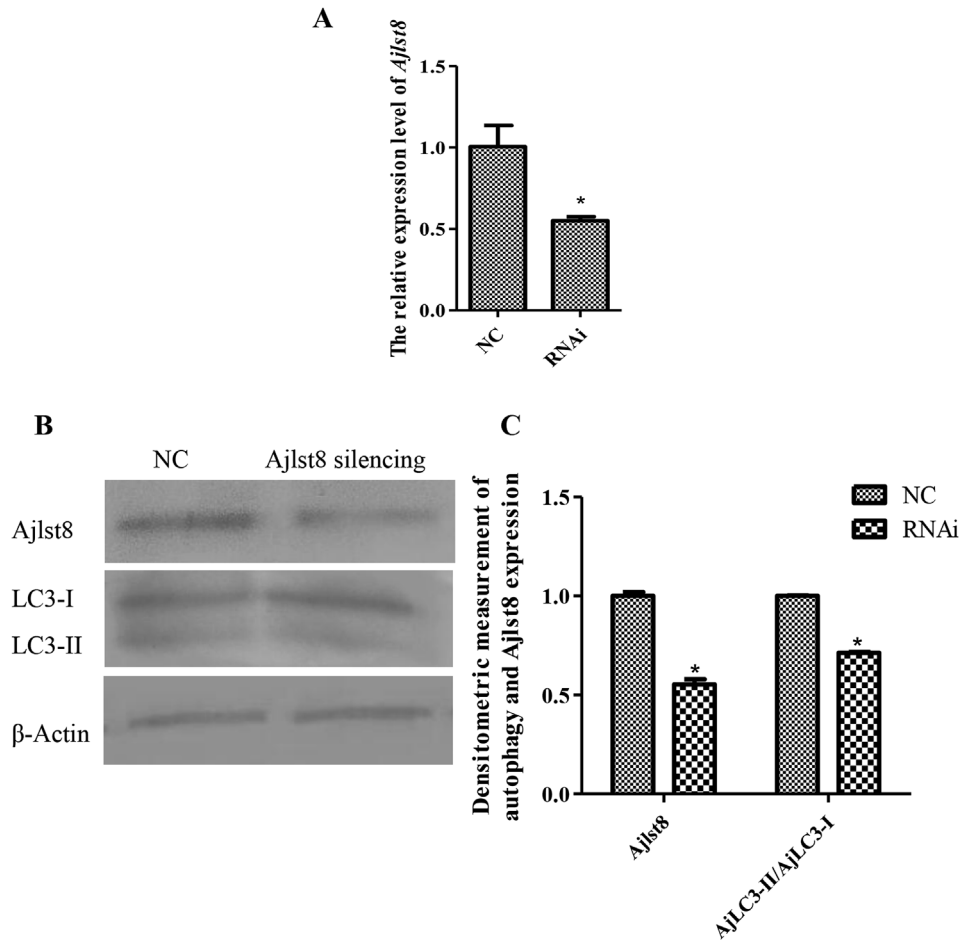

Fig. 7. Autophagy assay in Ajlst8 silencing via siRNA transfection in cultured coelomocytes. A: Silencing efficiency assay of Ajlst8 knockdown. B: Protein level of Ajlst8 and autophagy-related protein as determined via Western blotting. C: Statistical analysis of the expression levels of Ajlst8 and LC3-II/LC3-I. Values are expressed as mean ± SD ($n = 3$). Asterisks indicate significant differences: $^*P < 0.05$.

consistent with its positive regulatory roles in the immune response of *A. japonicus* upon pathogen challenge. Our results showed that *Ajlst8* mRNA expression in coelomocytes was considerably upregulated and reached the highest level at 6 h after challenge by *V. splendidus* (Fig. 5 A). During bacterial infection, autophagy may resist pathogen invasion, and consequently, helps clear cell-damaging bacterial irritants [43]. After *V. splendidus* infection, the upregulated expression of *Ajlst8* indicated its positive role in the autophagy response of *A. japonicus* coelomocytes against pathogen invasion. Simultaneously, numerous studies have shown that LPS is a powerful inflammatory stimulus that can activate immune response [44]. In this study, the expression level of *Ajlst8* in coelomocytes was significantly upregulated at 1 h compared with that in the control group after LPS mediation (Fig. 5 B). All these results supported the involvement of *Ajlst8* in innate immunity against pathogen invasion after bacterial infection and LPS exposure.

Autophagy is a fundamental process of innate immune response, and it plays a key role in a well-balanced inflammatory response and energy metabolism [45,46]. Autophagy flux is constant at basal levels. However, upon the introduction of different stimuli, including starvation, stress, and pathogen infection, the rate of autophagy flux can be enhanced. Furthermore, the autophagy capacity of a cell is directly proportional to lysosomal function and the efficiency of autophagosomes to fuse with lysosomes [47]. LC3 is a widely used marker for autophagosome detection in microscopy [48]. The relative amount of LC3-II/LC3-I is used to quantify autophagy activity in cells via immunoblot analysis [49,50]. In the present study, the autophagy of coelomocytes was significantly promoted in the LPS-mediated group. Under LPS exposure, the expression level of Ajlst8 was considerably upregulated, the ratio of LC3-II/LC3-I was remarkably increased, and the expression level of Ajlst8 in coelomocytes was upregulated. Our unpublished transmission electron microscope results also showed the accumulation of autophagy vacuoles in infected coelomocytes exposed to a pathogen. All these findings supported that Ajlst8 plays an important role in the autophagy process of sea cucumber under LPS exposure. When sea cucumber was challenged by pathogen or PAMP, the expression level of Ajlst8 was upregulated to induce autophagy in coelomocytes. Studies have reported that lst8 has no active site in mTORC1 and functions as a link between Kog1 and TOR [51]. Moreover, when lst8 is knocked out, the physiological response (e.g., DNA damage repair) elicited by mTORC1 will persist [52]. To address this issue, we assayed the mRNA and protein expression levels of autophagy under *Ajlst8* silencing condition. Compared with the untreated sea cucumber coelomocytes, the mRNA expression level of *Ajlst8* was significantly downregulated after specific RNAi. Meanwhile, the ratio of AjLC3-II/AjLC3-I in coelomocytes was slightly decreased after interference, and the autophagy degree was slightly weakened. Therefore, we speculate that the formation of autophagosomes and the increase of autophagy in the coelomocytes of sea cucumber are related to Ajlst8. However, this reaction may be simultaneously regulated by other subunits of mTORC1 (e.g., Kog1 and TOR), and the loss of Ajlst8 will slow down this reaction [53].

In summary, we identified and characterized the full-length cDNA sequence of *Ajlst8* from *A. japonicus* and investigated its roles in innate immunity. Although inconclusive, our findings suggest that *A. japonicus*

may use autophagy as a defense against pathogen infection, and the autophagy phenomenon is regulated by the subunit lst8 of mTORC1. Although this regulation is not same as the autophagy regulation of vertebrates, this study proves that Ajlst8 participates in the autophagy of *A. japonicus* and plays an important role in this process. Understanding the molecular details of how LPS mediation and *V. splendidus* infection engage autophagy will clarify the roles of autophagy in immunity and may aid in the rational design of effective therapeutics to control pathogen infection and treat diseases.

Acknowledgement

This work was financially supported by National Key R&D Program of China (2018YFD0901601, 2018YFD0900603), Zhejiang Provincial Natural Science Foundation (LZ19C190001), National Natural Science Foundation of China (31522059, 41576139), and the K.C. Wong Magna Fund in Ningbo University.

References

[1] M. Tsukada, Y. Ohsumi, Isolation and characterization of autophagy-defective mutants of Saccharomyces cerevisiae, FEBS (Fed. Eur. Biochem. Soc.) Lett. 333 (1993) 169–174.
[2] L. Qin, X. Wang, S. Zhang, S. Feng, L. Yin, H. Zhou, Lipopolysaccharide-induced autophagy participates in the control of pro-inflammatory cytokine release in grass carp head kidney leukocytes, Fish Shellfish Immunol. 59 (2016) 389–397.
[3] G.E. Mortimore, N.J. Hutson, C.A. Surmacz, Quantitative correlation between proteolysis and macro- and microautophagy in mouse hepatocytes during starvation and refeeding, Proc. Natl. Acad. Sci. U.S.A. 80 (1983) 2179–2183.
[4] P. Boya, F. Reggiori, P. Codogno, Emerging regulation and functions of autophagy, Nat. Cell Biol. 7 (2013) 713–720.
[5] T. Saitoh, N. Fujita, T. Yoshimori, S. Akira, Autophagy and innate immunity, Tanpakushitsu Kakusan Koso 53 (2008) 2279–2285.
[6] S. Ruf, A.M. Heberle, M. Langelaar-Makkinje, S. Gelino, D. Wilkinson, C. Gerbeth, J.J. Schwarz, B. Holzwarth, B. Warscheid, C. Meisinger, M.A. van Vugt, R. Baumeister, M. Hansen, K. Thedieckb, PLK1 (polo like kinase 1) inhibits MTOR complex 1 and promotes autophagy, Autophagy 13 (3) (2017) 486–505.
[7] H.J. Pan, X.P. Zhong, S. Lee, Sustained activation of mTORC1 in macrophages increases AMPKα-dependent autophagy to maintain cellular homeostasis, BMC Biochem. 17 (1) (2016) 14 (Rome).
[8] Y. Rabanal-Ruiz, E.G. Otten, V.I. Korolchuk, MTORC1 as the main gateway to autophagy, Essays Biochem. 61 (6) (2017) 565–584.
[9] E.A. Dunlop, A.R. Tee, MTOR and autophagy: a dynamic relationship governed by nutrients and energy, Semin. Cell Dev. Biol. 36 (2014) 121–129.
[10] L. Ma, Z. Chen, H. Erdjument-Bromage, P. Tempst, P.P. Pandolfi, Phosphorylation and functional inactivation of TSC2 by Erk implications for tuberous sclerosis and cancer pathogenesis, Cell 121 (2) (2005) 179–193.
[11] J. Huang, B.D. Manning, The TSC1-TSC2 complex: a molecular switchboard controlling cell growth, Biochem. J. 412 (2) (2008) 179–190.
[12] D.H. Kim, D.D. Sarbassov, S.M. Ali, R.R. Latek, K.V. Guntur, H. Erdjument-Bromage, P. Tempst, D.M. Sabatini, GβL, a positive regulator of the rapamycin-sensitive pathway required for the nutrient-sensitive interaction between raptor and mTOR, Mol. Cell 11 (4) (2003) 895–904.
[13] A. Adami, B. García-Alvarez, E. Arias-Palomo, D. Barford, O. Llorca, Structure of TOR and its complex with KOG1, Mol. Cell 27 (3) (2007) 509–516.
[14] H. Yang, D.G. Rudge, J.D. Koos, B. Vaidialingam, H.J. Yang, N.P. Pavletich, mTOR kinase structure, mechanism and regulation, Nature 497 (7448) (2013) 217–223.
[15] T. Dobrenel, C. Caldana, J. Hanson, C. Robaglia, M. Vincentz, B. Veit, C. Meyer, TOR signaling and nutrient sensing, Annu. Rev. Plant Biol. 67 (2016) 261–285.
[16] N. Mizushima, The role of the Atg1/ULK1 complex in autophagy regulation, Curr. Opin. Cell Biol. 22 (2) (2010) 132–139.
[17] Y. Kamada, T. Funakoshi, T. Shintani, K. Nagano, M. Ohsumi, Y. Ohsumi, Tor-mediated induction of autophagy via an Apg1 protein kinase complex, J. Cell Biol. 150 (6) (2000) 1507–1513.
[18] D.A. Guertin, D.M. Stevens, C.C. Thoreen, A.A. Burds, N.Y. Kalaany, J. Moffat, M. Brown, K.J. Fitzgerald, D.M. Sabatini, Ablation in mice of the mTORC components raptor, rictor, or mlst8 reveals that mTORC2 is required for signaling to Akt-FOXO and PKCalpha, but not S6K1, Dev. Cell 11 (6) (2006) 859–871.
[19] K. Kakumoto, J. Ikeda, M. Okada, E. Morii, C. Oneyama, MLST8 promotes mTOR-mediated tumor progression, PLoS One 10 (4) (2015) e0119015.
[20] X.H. Liang, S. Jackson, M. Seaman, K. Brown, B. Kempkes, H. Hibshoosh, B. Levine, Induction of autophagy and inhibition of tumorigenesis by beclin 1, Nature 402 (6762) (1999) 672–676.
[21] E. White, Deconvoluting the context-dependent role for autophagy in cancer, Nat. Rev. Canc. 12 (6) (2012) 401–410.
[22] L.J. Luo, J. Lu, A.L. Xu, Autophagy participates in innate immune defense in lamprey, Fish Shellfish Immunol. 83 (2018) 416–424.
[23] C.J. Kuo, M. Hansen, E. Troemel, Autophagy and innate immunity: insights from invertebrate model organisms, Autophagy 14 (2) (2018) 233–242.
[24] D. Voronin, D.A. Cook, A. Steven, M.J. Taylor, Autophagy regulates Wolbachia populations across diverse symbiotic associations, Proc. Natl. Acad. Sci. U.S.A. 109 (2012) 1638–1646.
[25] S. Shelly, N. Lukinova, S. Bambina, A. Berman, S. Cherry, Autophagy is an essential component of Drosophila immunity against vesicular stomatitis virus, Immunity 30 (4) (2009) 588–598.
[26] K. Jia, C. Thomas, M. Akbar, Q.H. Sun, B. Adams-Huet, C. Gilpin, B. Levine, Autophagy genes protect against Salmonella typhimurium infection and mediate insulin signaling-regulated pathogen resistance, Proc. Natl. Acad. Sci. U.S.A. 106 (34) (2009) 14564–14569.
[27] C.J. Lowe, Molecular genetic insights into deuterostome evolution from the direct-developing hemichordate Saccoglossus kowalevskii, Philos. Trans. R. Soc. Lond. Ser. B Biol. Sci. 363 (1496) (2008) 1569–1578.
[28] Fisheries Bureau of Ministry of Agriculture, China Fishery Statistical Yearbook, China Agriculture Press, Beijing, 2018.
[29] C.R. Hauck, M. Borisova, P. Muenzner, Exploitation of integrin function by pathogenic microbes, Curr. Opin. Cell Biol. 24 (5) (2012) 637–644.
[30] H. Deng, C. He, Z. Zhou, C. Liu, K. Tan, N. Wang, B. Jiang, X. Gao, W. Liu, Isolation and pathogenicity of pathogens from skin ulceration disease and viscera ejection syndrome of the sea cucumber, Aquaculture 287 (2009) 18–27.
[31] H. Liu, F. Zheng, X. Sun, X. Hong, S. Dong, B. Wang, X. Tang, Y. Wang, Identification of the pathogens associated with skin ulceration and peristome tumescence in cultured sea cucumbers, J. Invertebr. Pathol. 105 (3) (2010) 236–242.
[32] T.F. Smith, C. Gaitatzes, K. Saxena, E.J. Neer, The WD repeat: a common architecture for diverse functions, Trends Biochem. Sci. 24 (5) (1999) 181–185.
[33] T. Shintant, D.J. Klionsky, Autophagy in health and disease:a double-edged sword, Science 306 (5698) (2004) 990–995.
[34] X.J. Hu, T. Li, Y. Wang, Y. Xiong, X.H. Wu, D.L. Zhang, Z.Q. Ye, Y.D. Wu, Prokaryotic and highly-repetitive WD40 proteins: a systematic study, Sci. Rep. 7 (1) (2017) 10585.
[35] X.H. Wu, R.C. Chen, Y. Gao, Y.D. Wu, The effect of Asp-His-Ser/Thr-Trp tetrad on the thermostability of WD40-repeat proteins, Biochemistry 49 (47) (2010) 10237–10245.
[36] B.D. Rodgers, M.A. Levine, M. Bernier, C. Montrose-Rafizadeh, Insulin regulation of a novel WD-40 repeat protein in adipocytes, J. Endocrinol. 168 (2) (2001) 325–332.
[37] M. Moreau, M. Azzopardi, G. Clement, T. Dobrenel, C. Marchive, C. Renne, M.L. Martin-Magniette, L. Taconnat, J.P. Renou, C. Robaglia, C. Meyer, Mutations in the Arabidopsis homolog of lst8/GbetaL, a partner of the target of Rapamycin kinase, impair plant growth, flowering, and metabolic adaptation to long days, Plant Cell 24 (2) (2014) 463–481.
[38] D. Migliorini, S. Bogaerts, D. Defever, R. Vyas, G. Denecker, E. Radaelli, A. Zwolinska, V. Depaepe, T. Hochepied, W.C. Skarnes, J.C. Marine, Cop1 constitutively regulates c-Jun protein stability and functions as a tumor suppressor in mice, J. Clin. Investig. 121 (4) (2011) 1329–1343.
[39] C. González-Estévez, D.A. Felix, M.D. Smith, J. Paps, S.J. Morley, V. James, T.V. Sharp, A.A. Aboobaker, SMG-1 and mTORC1 act antagonistically to regulate response to injury and growth in planarians, PLoS Genet. 8 (3) (2012) e1002619.
[40] P.S. Gross, W.Z. Al-Sharif, L.A. Clow, L.C. Smith, Echinoderm immunity and the evolution of the complement system, Dev. Comp. Immunol. 23 (4–5) (1999) 429–442.
[41] T.D. Kanneganti, N. Ozören, M. Body-Malapel, A. Amer, J.H. Park, L. Franchi, J. Whitfield, W. Barchet, M. Colonna, P. Vandenabeele, J. Bertin, A. Coyle, E.P. Grant, S. Akira, G. Núñez, Bacterial RNA and small antiviral compounds activate caspase-1 through cryopyrin/Nalp3, Nature 440 (7081) (2006) 233–236.
[42] J.W. Pinkerton, R.Y. Kim, A.A. Robertson, J.A. Hirota, L.G. Wood, D.A. Knight, M.A. Cooper, L.A.J. O'Neill, J.C. Horvat, P.M. Hansbro, Inflammasomes in the lung, Mol. Immunol. 86 (2017) 44–55.
[43] V. Deretic, B. Levine, Autophagy balances inflammation in innate immunity, Autophagy 14 (2) (2018) 243–251.
[44] Y. Rosenfeld, Y. Shai, Lipopolysaccharide (Endotoxin)-host defense antibacterial peptides interactions: role in bacterial resistance and prevention of sepsis, Biochim. Biophys. Acta 1758 (9) (2006) 1513–1522.
[45] R.T. Netea-Maier, T.S. Plantinga, F.L. Veerdonk, J.W. Smit, M.G. Netea, Modulation of inflammation by autophagy: consequences for human disease, Autophagy 12 (2) (2016) 245–260.
[46] M.J. Czaja, W.X. Ding, T.M. Donohue, S.L. Friedman, J.S. Kim, M. Komatsu, J.J. Lemasters, A. Lemoine, J.D. Lin, J.J. Ou, D.H. Perlmutter, G. Randall, R.B. Ray, A. Tsung, X.M. Yin, Functions of autophagy in normal and diseased liver, Autophagy 9 (8) (2013) 1131–1158.
[47] D.J. Klionsky, et al., Guidelines for the use and interpretation of assays for monitoring autophagy, Autophagy 8 (4) (2012) 445–544.
[48] C. Otomo, Z. Metlagel, G. Takaesu, T. Otomo, Structure of the human ATG12-ATG5 conjugate required for LC3 lipidation in autophagy, Nat. Struct. Mol. Biol. 20 (1) (2013) 59–66.
[49] S. Oh, Y. Choi, J. Kim, C.C. Weihl, J. Ju, Quantification of autophagy flux using LC3 ELISA, Anal. Biochem. 530 (2017) 57–67.
[50] N. Mizushima, T. Yoshimori, B. Levine, Methods in mammalian autophagy research, Cell 140 (3) (2010) 313–326.
[51] T. Wang, R. Blumhagen, U. Lao, Y. Kuo, B.A. Edgar, Lst8 regulates cell growth via target-of-Rapamycin complex 2 (TORC2), Mol. Cell. Biol. 32 (12) (2012) 2203–2213.
[52] Y.X. Ma, Y. Vassetzky, S. Dokudovskaya, MTORC1 pathway in DNA damage response, Biochim. Biophys. Acta Mol. Cell Res. 1865 (9) (2018) 1293–1311.
[53] P.M. Wong, C. Puente, I.G. Ganley, X. Jiang, The ULK1 complex: sensing nutrient signals for autophagy activation, Autophagy 9 (2) (2013) 124–137.